Situation-dependent observation errors for AMSU-A tropospheric channels in the ECMWF forecasting system

Heather Lawrence, Niels Bormann, Enza Di Tomaso and Stephen English

ECMWF, Shinfield Park, Reading
RG2 9AX, United Kingdom
heather.lawrence@ecmwf.int

ABSTRACT

The Advanced Microwave Sounding Unit-A (AMSU-A) is a key satellite instrument used in numerical weather prediction systems around the world. In order to assimilate AMSU-A data, observation errors must be defined. In the ECMWF system each AMSU-A channel is currently assigned a constant observation error. However the observation errors should include forward model error, which will depend on the state of the atmosphere and surface. Here we present a study where observation errors for the surface- and cloud-sensitive channels were allowed to vary with surface type (land, sea, sea-ice, snow cover), sensitivity to the surface (surface-to-space transmittance) and the liquid water path, in order to account for errors in the forward model due to emissivity errors and undetected cloud/precipitation. We developed the new observation errors and ran assimilation trials using these new situation-dependent values. We also investigated extending the coverage with these new observation errors by relaxing screening over high orography and by relaxing the cloud screening. First results showed that the new observation errors had a neutral impact on forecast scores when no new data were added but there was a reduction in the standard deviation of background departures for ATMS when the AMSU-A cloud screening was relaxed, which was encouraging.

1 Introduction

At ECMWF, radiances from AMSU-A temperature sounding channels are actively assimilated from instruments aboard 6 different polar-orbiting satellites, providing a very good global coverage. The tropospheric channels are particularly important for weather prediction but they suffer from cloud contamination and uncertainties in surface temperature and emissivity since they are surface-sensitive, and this will produce errors in the forward model. When assimilating the radiances of these channels we must define observation errors, which should include this forward model error as well as the instrument noise. Currently, fixed values of 0.28 K and 0.20 K are applied for channels 5 and 6 - 7 respectively. Here we present a method for calculating situation - dependent observation errors which depend on the surface temperature, surface-to-space transmittance and liquid water path. The approach follows methods outlined by [Candy, 2010], [Lean et al., 2012], [Di Tomaso et al., 2013] but includes a non-constant liquid water path error. First results from assimilation trials using these observation errors are also shown.

2 Situation Dependent Observation Errors

The total observation error, σ_o, for the lower peaking channels of AMSU-A can be written as a summation of the instrument noise, σ_N, and the forward model errors which for surface- and cloud-sensitive channels includes a surface term, $\sigma_{surface}$, and a liquid water path (lwp) term. Thus σ_o can be expressed as follows:

$$\sigma_o^2 = \sigma_{surface}^2 + \sigma_{lwp}^2 + \sigma_N^2 \tag{1}$$

The σ_{lwp}-term arises as we currently assimilate AMSU-A using a clear-sky radiative transfer model. To limit the effect of cloud contamination, clear-sky observations are identified in the ECMWF system in the following way: the absolute value of FG-departures in a window channel needs to be below a certain threshold (using channel 3 and a threshold of 3 K over ocean, and channel 4 and a threshold of 0.7 K over land), and an observation-based estimate of the lwp needs to be below 0.3 kg/m^2 over oceans. Attempts at using the tropospheric AMSU-A channels in all-sky conditions have so far not been successful [Geer et al., 2012].

The surface and lwp terms of (1) were calculated as follows.

2.1 Surface Errors

Currently the land and sea-ice surface emissivities used for AMSU-A sounding channels are retrieved prior to the assimilation from the radiances of a window channel (channel 3), following the method developed by [Karbou et al., 2006]. Sea surface emissivities are calculated from the FASTEM model. The forward model error due to emissivity errors, $\sigma_{surface}$, can be approximated to ([English, 2008]):

$$\sigma_{surface} \approx T_S \tau^2 \sigma_\varepsilon, \tag{2}$$

where T_S is the skin temperature, τ is the surface-to-space transmittance and σ_ε is the surface emissivity error. Note that in (2) we assume an isothermal atmosphere and that the atmospheric temperature may be approximated to the skin temperature, T_s. We do not consider contributions from errors in the skin temperature because, in the ECMWF 4D-Var assimilation system, the skin temperature is retrieved during the analysis as a sink variable.

For cloud-free data (1) can therefore be rewritten as:

$$\sigma_o^2 \approx \left(T_S \tau^2 \sigma_\varepsilon\right)^2 + \sigma_N^2, \tag{3}$$

The emissivity errors, σ_ε, were estimated for different surface types by fitting (3) to the mean-square background departures as a function of binned first guess $\left(T_s \tau^2\right)^2$ values for channel 5 AMSU-A. This was done for all data which had been filtered for cloud-contamination. Cloudy data were identified using the standard IFS quality control, with a tighter check on clouds over ocean excluding data with lwp $>$ 0.05 kg/m^2. Noise terms, σ_N, were simultaneously calculated as the intercept. Values were obtained for σ_ε for ocean, sea-ice, snow-covered land and snow-free land and these are given in table 1. Previously [Di Tomaso et al., 2013] calculated values for different land surface types (forest, desert, etc.) but, with the exception of snow cover, these values were all very similar. We therefore decided to combine the land surfaces into two types only: snow-free and snow-covered.

Table 1: Emissivity errors for different surface types

Surface Type	σ_ε
Ocean	0.015
Snow - free land	0.022
Snow - covered land	0.050
Sea-ice	0.050

We checked the validity of values found for σ_ε for different surface types by calculating also the standard deviation of retrieved emissivities for these surfaces. This produced similar to values to those shown in table 1.

2.2 Liquid Water Path Errors

Errors arising from neglecting cloud-contributions in the radiative transfer are parameterised empirically using an estimate of the liquid water path in the observations. The liquid water path is calculated over ocean from AMSU-A window channels 1 and 2, following the method of [Grody et al., 2001]. The standard deviation of background departures gives us a good indication of the observation errors for AMSU-A channels 5 - 7 and so we can look at how they vary with liquid water path (over ocean). Figure 1 shows that the standard deviation of background departures increases approximately quadratically for channels 5 and 6 and in a linear manner for channel 7. We therefore decided to model the liquid water path error terms as follows:

channels 5 and 6:

$$\sigma_{lwp} = Alwp^2 + Blwp, \tag{4}$$

channel 7:

$$\sigma_{lwp} = Alwp, \tag{5}$$

for some constants A and B. We can thus rewrite the observation error due to instrument noise and liquid water path terms as:

channels 5 and 6:

$$\sigma_o^2 = \sigma_N^2 + \left(Alwp^2 + Blwp\right)^2 \tag{6}$$

channel 7:

$$\sigma_o^2 = \sigma_N^2 + (Alwp)^2 \tag{7}$$

Applying a quadratic fit has some physical basis, since the cloud liquid water will affect the τ term (surface-to-space transmittance) in the radiative transfer equations, which takes the form of an exponential. The additional exponential term could be approximated to a quadratic in a Taylor expansion. However it is worth noting that the first guess departures are also affected by scattering of ice clouds, snow and rain which are likely to be correlated to some extent to cloud liquid water. Some of the dependency of first guess departures on the cloud liquid water path may be due to this correlation to scattering, and this correlation may even dominate over cloud liquid water effects particularly for channels 6 and 7.

Assuming that the observation errors are dominated by liquid water path errors over ocean, we calculated a best fit of (6) and (7) where the standard deviation of background departures were used as a proxy for σ_o, in order to obtain values for constants A, B and σ_N . We found the following best fits for σ_{lwp}, which are also plotted in figure 1 for an instrument noise of 0.25 K for channel 5 and 0.20 K for channels 6 and 7:

channel 5:

$$\sigma_{lwp} = 0.2lwp^2 + 0.79lwp, \tag{8}$$

channel 6:

$$\sigma_{lwp} = 0.54lwp^2 + 0.30lwp, \tag{9}$$

channel 7:

$$\sigma_{lwp} = 0.20lwp. \tag{10}$$

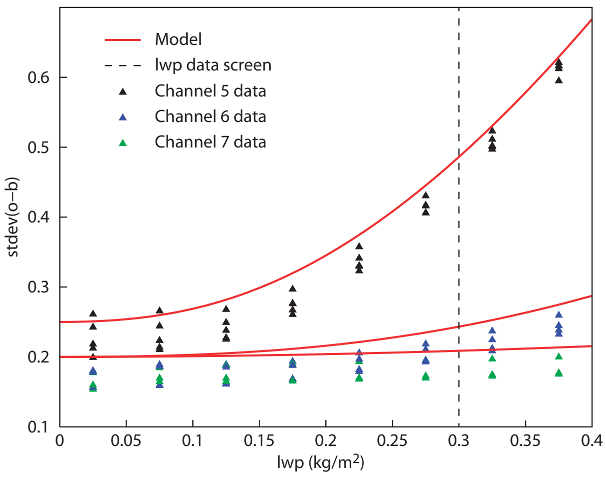

Figure 1: Standard deviation of background departures as a function of binned liquid water path values for channels 5, 6 and 7 of AMSU-A. The different points indicate different satellites. The red lines show the best fits and the black dashed line indicates the liquid water path value above which data are not used for channels 5 or 6.

Note that over land we currently do not attempt to model the error contribution from neglecting cloud effects in the observation operator.

2.3 Instrument noise

When calculating the best fits for the surface and liquid water path errors we simultaneously calculated noise terms for each satellite instrument (in sections 2.1 and 2.2), as the intercept values. These varied for different satellite-channel combinations but it was decided to keep a constant value for each satellite. A fixed value of 0.25 K was used for channel 5 instrument noise term, σ_N, and 0.20 K for channels 6 and 7. These values are the highest found for the satellite-channel combinations.

3 First assimilation trials

Situation-dependent observation errors allow us to weight the data in a more accurate manner. This also means that they may allow us to introduce more data over areas which are currently excluded from the assimilation, as they showed higher forward model errors that were previously not accounted for. This includes areas with high orography, the South Pole or areas with weak cloud-contamination.

The following experiments were run:

- Control: The operational 4D-VAR model (version 40R1) at T511 with 137 vertical levels, including some contributions to cycle 40R2. Observation errors for AMSU-A channels 5 - 7 are constant.
- Situation-dependent observation errors: The same as the control with observation errors changed to (1) combined with (2) and (8) - (10) for channels 5 - 7.
- Extended coverage over cloudy regions: The same as Situation-dependent observation errors with the window channel background departure check removed over ocean and replaced by a scatter

index check (keeping data with scatter index < -30K). As with the control, data are also not used for channels 5 and 6 if the liquid water path exceeds 0.3 kg/m^2.

- Extended coverage over high orography: The same as Situation-dependent observation errors with channel 5 coverage extended over sea-ice in the Southern Hemisphere (it is currently blacklisted operationally) and data for channels 5 - 7 introduced over high orography. Instead, we reject data with observation errors larger than 0.35 for channel 5 and 0.28 for channel 6 (2 x the noise).

Each experiment was performed over 2 months for the period 15 June 2013 - 14 August 2013.

4 Results

The new observation errors down-weight data with a higher liquid water path, a higher surface-to-space transmittance and/or a higher surface temperature. Equally data with a lower liquid water path, or surface sensitivity have more weight. Figure 2 shows the new observation errors for channel 5 for the 'Situation dependent observation errors' experiment. In this figure we can see that for channel 5 the observation errors are higher in the centre of the swath, where the observation angle is close to nadir and surface-to-space transmittance is higher. There are also higher values over sea-ice due to a higher emissivity error and higher values in areas of high liquid water path which pass the cloud-screening, such as over the Southern hemisphere ocean. Note that in the tropics data with high liquid water paths generally do not pass the current cloud screening.

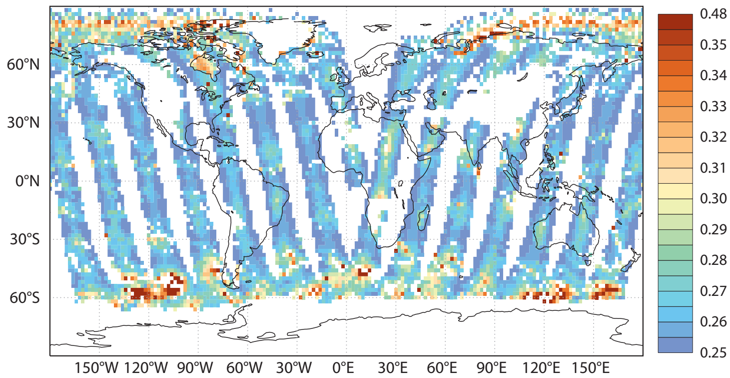

Figure 2: Observation errors for Metop-B AMSU-A channel 5 for 15 June 2013. The edges of the scanline have lower observation errors due to lower surface-to-space transmittance. Higher observation errors over land, sea-ice and high liquid water path can also be seen.

The extended coverage experiments used more data, as shown in figure 3:

Results of the experiments with the new situation-dependent observation errors indicated a generally neutral impact on globally averaged forecast scores. For example the forecast scores for 500hPa geopotential height are shown in figure 4.

Extending the coverage by relaxing the cloud-screening produced a mainly neutral impact on forecast scores (see figure 4) but reduced the standard deviation of background departures for ATMS, as shown in figure 5. This latter result is encouraging since ATMS data are strongly screened for cloud and so the new AMSU-A data are in agreement with the non-cloudy ATMS data.

Extending the coverage over high orography changed the mean forecast fields over the South Pole and Greenland, and the forecast impact over Antarctica is mainly negative. The positive scores below 500hPa shown in figure 6 are deceptive because the land is higher than this over Antarctica and so these scores

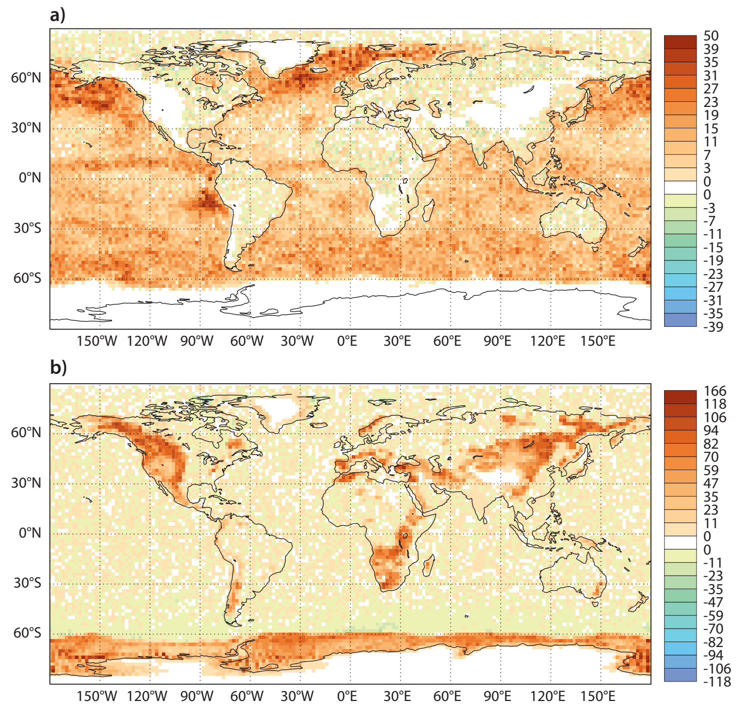

Figure 3: Change in the number of data used for MetOp-B AMSU-A channel 5 (1 month average) between a) Extended coverage over cloudy regions experiment and control and b) Extended coverage over high orography and control

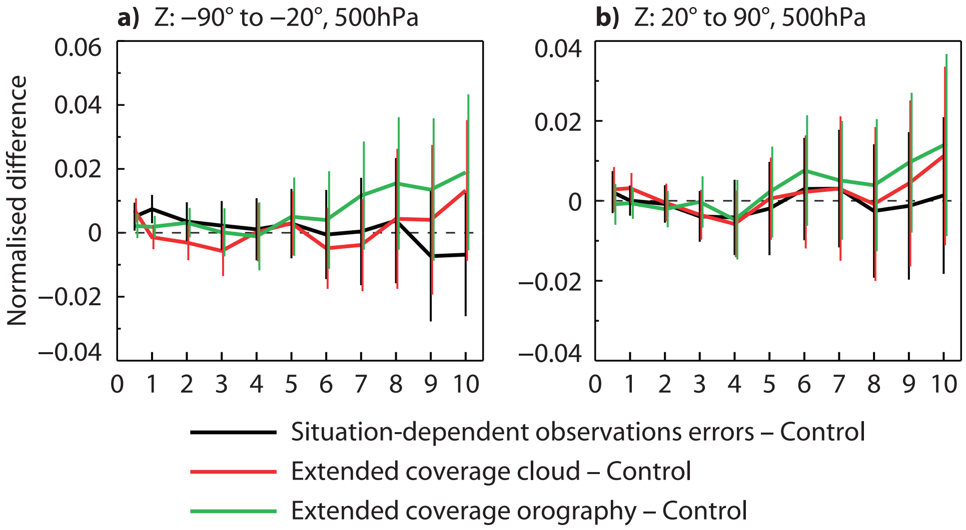

Figure 4: Normalised difference in the root mean square forecast error for 500 hPa geopotential as a function of forecast day (x axis). Values are averaged for 2 months over a) Northern hemisphere extra-tropics and b) Southern hemisphere extra-tropics. Error bars indicate 95 % confidence intervals.

do not have meaning. More work is required to attribute the impact to either the introduction of data over Antarctica or over the sea-ice. Elsewhere, the use of the additional data leads to a neutral to slightly positive impact on forecast scores in the Northern hemisphere, as shown in figure 6. This is encouraging as it may suggest improvements due to the less restricted orography screening in these areas.

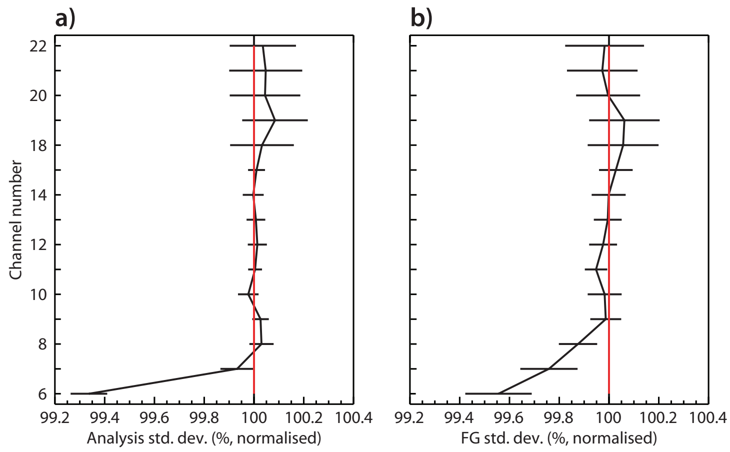

Figure 5: Standard deviation of a) analysis departures and b) background departures for the ATMS instrument (averaged globally) of the Extended coverage over cloudy regions normalised by the values of the control experiment.

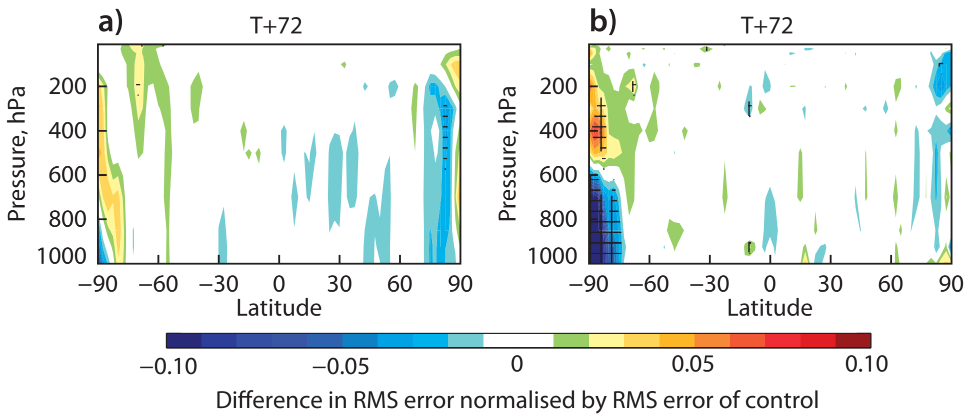

Figure 6: Change in the root mean square day 3 geopotential (left) and temperature forecasts (right) minus analysis between the extended coverage over orography experiment and control as a function of latitude (x axis) and pressure (y axis). Blue indicates a reduction in day 3 forecast error and red an increase.

5 Conclusions

New situation-dependent observation errors were calculated for AMSU-A channels 5 - 7 and these were tested in assimilation trials lasting 2 months. The new observation errors appeared to show neutral impact when the same cloud and orography screening was used. However when the cloud screening was relaxed the standard deviation of background departures was reduced for ATMS, indicating that the new data used for AMSU-A reinforced the ATMS data which is strongly screened for cloud. This is encouraging. Introducing new data by relaxing the orography screening led to mainly neutral results but with some small improvement in the geopotential forecast over the Northern Hemisphere.

Further experimentaton over longer periods and different seasons is required to corroborate our findings.

Acknowledgements

Heather Lawrence is funded by the EUMETSAT fellowship programme. Anabel Bowen is gratefully acknowledged for her help editing the figures.

References

[Candy, 2010] Candy, B. (2010). Results of applying variable observation errors to atovs part 1: Mainly surface error terms. personal communication.

[Di Tomaso et al., 2013] Di Tomaso, E., Bormann, N., and English, S. (2013). Assimilation of ATOVS radiances at ECMWF: third year EUMETSAT fellowship report. *available online: http://www.ecmwf.int/publications/library/do/references/show?id=90804*, 26pp.

[English, 2008] English, S. (2008). The importance of accurate skin temperature in assimilating radiances from satellite sounding instruments.

[Geer et al., 2012] Geer, A., Bauer, P., and English, S. (2012). Assimilating AMSU-A temperature sounding channels in the presence of cloud and precipitation. *ECMWF Tech. Memo.*, 670.

[Grody et al., 2001] Grody, N., Zhao, J., Ferraro, R., Weng, F., and Boers, R. (2001). Determination of precipitable water and cloud liquid water over oceans from the NOAA 15 advanced microwave sounding unit. *J. Geophys. Res.*, 106:2943–2953.

[Karbou et al., 2006] Karbou, F., Gerard, E., and Rabier, F. (2006). Microwave land emissivity and skin temperature for amsu-a and -b assimilation over land. *Q.J.Roy.Met.Soc.*, 132:2333–2355.

[Lean et al., 2012] Lean, K., Candy, B., Pavelin, E., and Sreerekha, T. (2012). Results of applying variable observation errors to atovs: Winter trial and results. personal communication.